Mextram Modeling of Si/SiGe Heterojunction Phototransistors

F. Yuan[1], Z. Pei[3], J. W. Shi[3], S. T. Chang[2], and C. W. Liu[1,3]
[1]Department of Electrical Engineering and Graduate Institute of Electronics Engineering,
National Taiwan University, Taipei, Taiwan, R. O. C.
[2]Department of Electronic Engineering, Chung Yuan Christian University, Taiwan, R. O. C.
[3]ERSO/ITRI, Hsinchu, Taiwan, R. O. C.
[3]E-mail: chee@cc.ee.ntu.edu.tw

To integrate the phototransistor into the receiver circuit for optical communication, not only the compatible process is pre-requisite [1], but also the device model is required for circuit simulation. The designed nkT base current (depletion region recombination current at B-E junction) can increase the bandwidth of the phototransistor and provide a possible bias margin for avalanche gain. Therefore, a modified Mextram model is proposed for the HPT simulation.

The cross section of the modeled Si/SiGe HPT is shown in Fig. 1, and the HPT is essentially a 4 terminal device, including E, B, C, and substrate contact (S). The MQW device has multiple quantum wells between the base and collector, and the regular device has not. The wavelength of the photo-excitation is 850nm. The substrate contact can drain the photo-generated holes when the light input is off, and has an important effect on HPT speed. The Mextram-based HPT model (Fig. 2) includes (1) voltage controlled current sources $I_{ph}(V_{CB})$ and $I_{sub}(V_{SC})$ to model the photocurrent at B-C and C-S junctions; (2) a light input subcircuit (R1, C1) models the initial time constant of impulse response by considering the current path of photo-generated holes to substrate and/or emitter with a partition ratio of r and discharge times τ_{sub} and $\tau_{C\text{-}B}$ for substrate path and emitter path, respectively, and (3) R_{nkT} and C2 are used to model the time constant at the tail of impulse response by considering the nkT recombination of photo-generated holes (Fig. 3). Note that the DC hole back injection current is modeled by intrinsic Mextram model. The impulse response with an open substrate has a very large time constant (~1.3ns), and can be modeled by letting r=0 in Fig. 2 (inset of Fig. 3). The Gummel plots of both the MQW and regular devices can be easily modeled by the intrinsic Mextram model (Fig. 4). The breakdown voltage BV_{CE} dependence on the nkT base current is modeled in Fig. 5. The lower current gain (β) yields a higher BV_{CEO} to meet the breakdown criteria, β(M-1)=1, where M, the multiplication factor, increases as V_{CB} increases. The common emitter characteristics in a log I_C scale have to be modeled by our modified Mextram model (Fig. 6) with R_C-limited avalanche photocurrent and V_{CB} controlled photocurrent I_{ph}. Note that the regular device has a strong nkT current to increase the speed and have an avalanche gain region. Since the both depletion region width and impact ionization rate increase as V_{CB} (reverse bias) increases, the photocurrent is a function of V_{CB}, and can be modeled by a simple linear approximation and an empirical equation (Fig. 7). This V_{CB} controlled photocurrent also leads a smaller Early voltage as compared to the constant I_B input at the similar I_C (Fig. 8). Similar Early voltage reduction is also observed in the regular device (Fig. 9) with shorted E and S. But the substrate contact shorted with the emitter contact enables the photocurrent I_{sub} to conduct, and the I_C has an extra component I_{sub} under light exposure (Fig. 9). To confirm this, the regular device under inverse active region (negative V_{CE}) has different polarity of I_C for dark and light exposure condition (Fig. 10). The I_C-V_{CE} simulation curves for regular devices (Fig. 11) and MQW devices (Fig. 12) are very close to the experiment data, indicating the accurate modeling for the DC characteristics. Note that the regular device has a larger I_{sub} and yields a larger offset current at V_{CE}=0V, as compared to the MQW device.

In conclusions, the Mextram model is suitable for HPT modeling. The impact ionization can get an extra gain in the optoelectronic conversion. The nkT base recombination current can increase the HPT speed, and can be well-modeled in our proposed modified Mextram model.

[1] Z. Pei et. al. IEDM Tech. Dig. p.297-300, 2002.

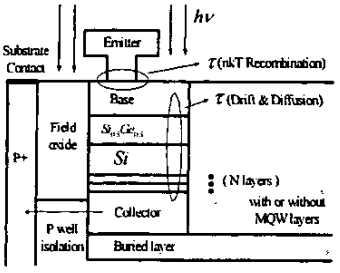

Fig. 1. Cross section of the Si/SiGe HPT. For MQW devices, the MQW is sandwiched between base and collector. For regular devices, there is no such MQWs.

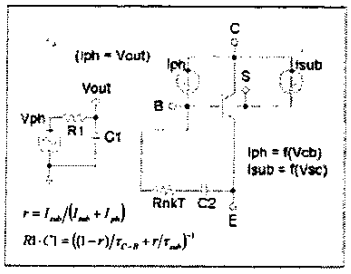

Fig. 2. The equivalent circuit of HPT used in SPICE. The photocurrent is modeled as the two current sources at collector-base and collector-substrate junction. They are function of V_{CB} and V_{SC}, respectively.

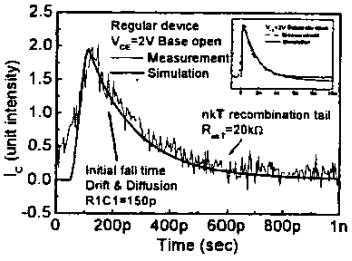

Fig. 3. The impulse response of a regular device. The initial fall time is due to the drift and diffusion of photo-generated holes. The tail is due to the nkT recombination. The inset is the wider impulse response with open substrate.

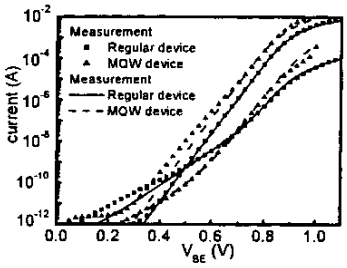

Fig. 4. The measured and the simulated Gummel plot in the dark. The base-collector bias is zero volts.

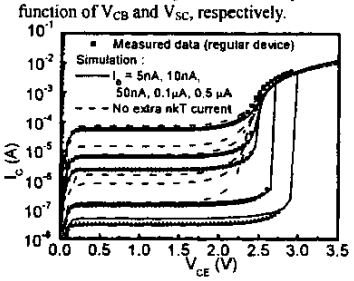

Fig. 5. The simulated and measured common emitter output characteristics with constant base currents input. The BV_{CE} would be almost constant if there were no such nkT component at BE junction. The breakdown voltage decreases as I_B increases.

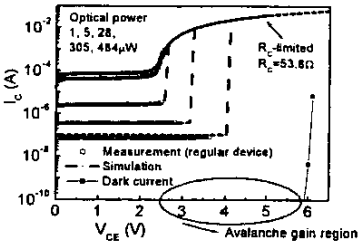

Fig. 6. The photocurrent of the regular device is simulated in output characteristics (in base open mode) with measured data. It shows the HPT can be operated at avalanche gain region to have an extra gain. The avalanche photocurrent is R_C-limited. The R_C is only 53.8Ω, but it can not be neglected at high avalanche current.

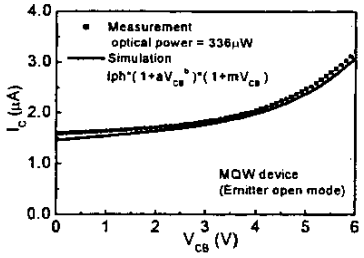

Fig. 7. The simulated collector current as a function of collector-base bias in emitter open mode with measured data. The linear approximation has a good agreement with measurement when the device is operated below the avalanche multiplication.

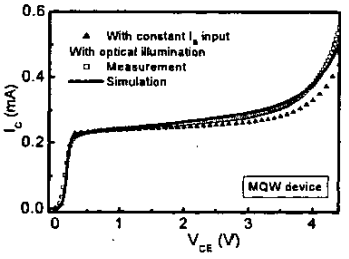

Fig. 8. Common emitter output characteristics for MQW device. The HPT device was measured with constant base current (1.45 μ A) and with optical illumination at 336 μ W (in base open mode).

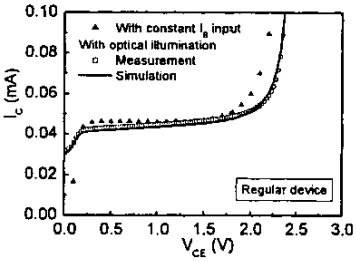

Fig. 9. Common emitter output characteristics for regular device. The device was measured with constant base current (0.4 μ A) and with optical illumination at 305 μ W (in base open mode).

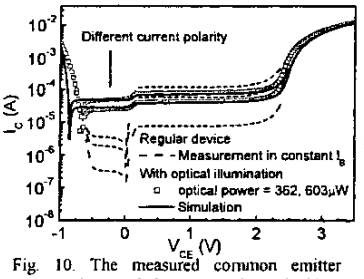

Fig. 10. The measured common emitter output characteristics at various incident optical powers in base open mode and at various constant base currents input. A different current polarity occurs at negative V_{CE} for the dark and light exposure conditions.

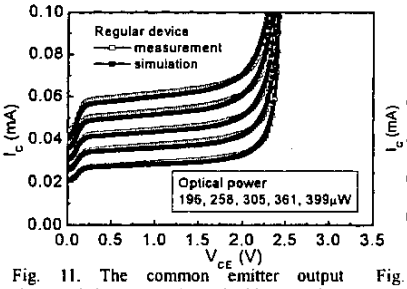

Fig. 11. The common emitter output characteristics at various incident optical powers in base open mode for the regular device.

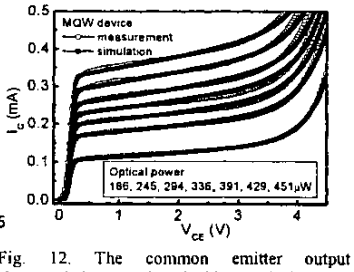

Fig. 12. The common emitter output characteristics at various incident optical powers in base open mode for the MQW device.